Structure, Vol. 11, 637–649, June, 2003, ©2003 Elsevier Science Ltd. All rights reserved. DOI 10.1016/S0969-2126(03)00093-5

Structure of the Coiled-Coil Dimerization Motif of Sir4 and Its Interaction with Sir3

Ju-Fang Chang,[1] Brian E. Hall,[1] Jason C. Tanny,[2] Danesh Moazed,[2] David Filman,[1] and Tom Ellenberger[1,*]

[1]Department of Biological Chemistry and Molecular Pharmacology and
[2]Department of Cell Biology
Harvard Medical School
240 Longwood Avenue
Boston, Massachusetts 02115

Summary

The yeast silent information regulators Sir2, Sir3, and Sir4 physically interact with one another to establish a transcriptionally silent state by forming repressive chromatin structures. The Sir4 protein contains binding sites for both Sir2 and Sir3, and these protein-protein interactions are required for gene silencing. Here, we report the X-ray structure of the coiled-coil dimerization motif within the C-terminus of Sir4 and show that it forms a stable 1:1 complex with a dimeric fragment of Sir3 (residues 464–978). We have identified a cluster of residues on the surface of the Sir4 coiled coil required for specific interactions with Sir3. The histone deacetylase Sir2 can also bind to this complex, forming a ternary complex with the truncated Sir3 and Sir4 proteins. The dual interactions of Sir4 with Sir3 and Sir2 suggest a physical basis for recruiting Sir3 to chromatin by virtue of its interactions with Sir4 and with deacetylated histones in chromatin.

Introduction

In higher organisms, the regulation of gene expression is governed locally by *cis*-acting transcription factors that bind to the regulatory elements of individual genes and, more generally, by the regional inactivation of chromosomal domains through the formation of repressive heterochromatin structures. The inaccessibility of heterochromatin to DNA binding factors and enzymes creates large stretches of the genome that are transcriptionally silent and resistant to genetic rearrangements (Gartenberg, 2000; Gasser and Cockell, 2001; Moazed, 2001). These silent tracts can be epigentically inherited, and they serve to prevent recombination or degradation at telomeres and the pericentric regions of chromosomes.

Extensive studies of gene silencing in the budding yeast *Saccharomyces cerevisiae* have revealed some of the generalized mechanisms for the formation of heterochromatin in more complex organisms. Although heterochromatin in yeast (referred to as silent chromatin) occurs in a few, select regions of the genome and includes protein components that have no obvious counterpart in mammalian cells, many of its functional properties are identical to those of mammalian heterochromatin (Moazed, 2001). Silent chromatin is established in *S. cerevisiae* at the mating type loci (*HML* and *HMR*) and at telomeres by the Sir (*s*ilent *i*nformation *r*egulator) proteins Sir2, Sir3, and Sir4 and at ribosomal DNA by Sir2 in combination with other factors. Deletion of any of these genes abolishes silencing at the *HM* loci and at telomeres (Aparicio et al., 1991; Rine and Herskowitz, 1987). The generation of silent chromatin is a multistep process that requires passage through the S phase of the cell cycle (Kirchmaier and Rine, 2001; Li et al., 2001; Miller et al., 1984). It involves a nucleation event followed by the spreading of the silencing factors along the DNA to distal regions of the chromosome. The spreading of the Sir protein complex causes the compaction of the nucleosomal arrays, making the DNA less accessible in the silent chromatin.

Silencing at telomeres is nucleated by the transient recruitment of the constitutively formed Sir2-Sir4 complex by the Ku heterodimer (Ku70/Ku80), ORC1, and Rap1 (Moazed et al., 1997; Moretti et al., 1994; Moretti and Shore, 2001). Sir2 is a NAD-dependent protein deacetylase that is conserved throughout the eukarya (Imai et al., 2000; Landry et al., 2000; Smith et al., 2000). Sir2 couples the deacetylation of protein substrates with the conversion of NAD to O-acetyl-ADP-ribose by an ADP ribosyl transfer mechanism (Tanner et al., 2000; Tanny and Moazed, 2001). In the current model of DNA silencing, Sir4 is the seminal factor that brings Sir2 to the nucleosomes to initiate the deacetylation of the N-terminal tails of histones H3 and H4 (Hoppe et al., 2002; Luo et al., 2002; Rusche et al., 2002). After nucleation, Sir3 is recruited by the Sir2-Sir4 complex to begin the spread of silent chromatin to more distal regions of the chromosome. The recruitment of Sir3 is thought to be the pivotal step that stabilizes the interaction of the silencing proteins with chromatin, so that spreading of the Sir protein complex can occur. Spreading involves further rounds of histone deacetylation by Sir2-Sir4 and then recruitment of Sir3. The Sir3 protein binds to both Sir4 and the hypoacetylated N-terminal tails of histones H3 and H4 (Hecht et al., 1995; Moazed et al., 1997; Moretti et al., 1994). The initial recruitment of Sir3 to the nucleation site for silencing does not require the enzymatic activity of Sir2, whereas the spreading of silent chromatin depends upon the Sir2-catalyzed deacetylation of histones (Hoppe et al., 2002; Luo et al., 2002; Rusche et al., 2002). This observation supports the notion that the initial recruitment of Sir3 occurs by its direct interaction with Sir4 and that spreading of the Sir protein complex along chromatin involves the binding of Sir3 to hypoacetylated histone tails. The cellular levels of the Sir3 protein are the limiting factor for the spread of silent chromatin in vivo (Hecht et al., 1996; Renauld et al., 1993). Together these data suggest a model in which nucleation by the Sir2-Sir4 complex is followed by the recruitment of Sir3, which functions as a lynchpin for the initiation and spreading of silent chromatin through

*Correspondence: tome@hms.harvard.edu

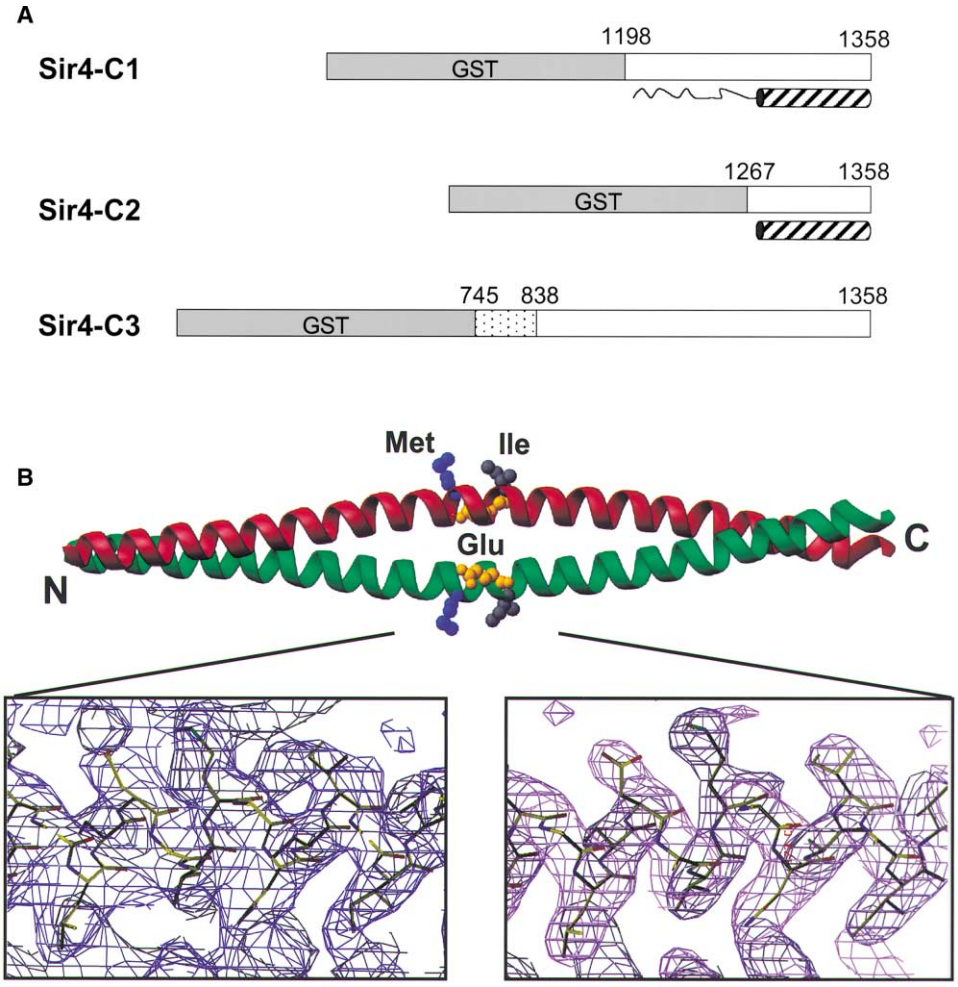

Figure 1. The Coiled-Coil Domain of Sir4 Mediates Dimerization and Interactions with Other Proteins

(A) N-terminally truncated Sir4 proteins were expressed as GST fusions for protein purification and protein interaction assays. The C-terminal half of the Sir4 protein (residues 745–1358) contains binding sites for Sir2 and Sir3. The Sir4-C1 protein (residues 1198–1358) that was crystallized has been shown to interact with a number of other proteins involved in gene silencing. Only 76 residues at the C terminus of Sir4-C1 are well ordered in the crystal, and they form a dimeric coiled coil that alone efficiently binds to Sir3 (cf. Figure 4).

(B) Ribbon diagram of the Sir4 coiled-coil dimer with the experimentally phased (left) and $2F_o - F_c$ omit (right) electron density maps contoured at 1.0 σ shown in the region of the Sir3 binding site. The figure was generated with the program RIBBONS (Carson, 1997). The side chains of residues that are required for efficient interaction with Sir3 are shown. They include M1307 (blue), E1310 (orange), and I1311 (gray) (cf. Figure 5).

physical interactions with Sir4 and histones, respectively.

The C-terminal 161 residues of Sir4 encompassed by the Sir4-C1 peptide (residues 1198–1358; Figure 1A) are dispensable for assembly of the Sir2-Sir4 complex, but absolutely essential for the recruitment of Sir3 to silencing complexes. Overexpression of Sir4-C1 disrupts silencing in vivo (Ivy et al., 1986), and this phenotype is suppressed by the overexpression of Sir3 (Marshall et al., 1987). Furthermore, deletion of the C-terminal region of Sir4 causes a loss of silencing at the *HM* loci and at telomeres (Kennedy et al., 1995). A direct, physical interaction of the Sir4-C1 domain with Sir3 has been demonstrated in yeast cell extracts (Moazed et al., 1997). Longer fragments of the Sir4 protein interact with Sir3 less efficiently, if at all, suggesting that the N-terminal region of Sir4 may obscure its C-terminal domain and prevent interactions with Sir3. The observation that most of the Sir3 protein in yeast cell extracts is not complexed to Sir4 (Moazed et al., 1997; Strahl-Bolsinger et al., 1997) might be explained by a block of the Sir3 binding site caused by the N-terminal region of Sir4. In light of the importance of Sir4-Sir3 complex formation for gene silencing, it seems likely that some other factor(s) can transiently expose the C terminus of Sir4 for interactions with Sir3 in vivo (Moazed et al., 1997).

In addition to its role in recruiting Sir3 to silent chromatin, the C-terminal domain of Sir4 has been implicated in many other distinct, yet related, processes. The Sir4-C1 region and Sir3 are both required for the normal positioning of telomeres within the yeast nucleus (Cockell et al., 1995; Marshall et al., 1987; Palladino et al., 1993). A direct interaction between the telomere binding protein RAP1 and the C-terminal domain of Sir4 has

been detected in vitro (Cockell et al., 1995) and in yeast two-hybrid assays (Moretti et al., 1994; Moretti and Shore, 2001). It has also been reported that the Sir proteins relocalize from telomeres to the sites of double-strand DNA breaks along with the Ku heterodimer (Martin et al., 1999; McAinsh et al., 1999; Mills et al., 1999; Tsukamoto et al., 1997). Although the role(s) of the Sir proteins at double-strand breaks are unknown, the direct interaction of the yeast Ku homolog Hdf1 with the C-terminal domain of Sir4 in a yeast two-hybrid experiment (Tsukamoto et al., 1997) suggests a specific role in the detection or repair of DNA double-strand breaks. The Sir4-C1 domain has also been shown to associate tightly with UBP3, a yeast deubiquitinating enzyme, raising the possibility that the activities of Sir protein complexes could be regulated in vivo by ubiquitination and proteasomal degradation of the Sir proteins (Moazed and Johnson, 1996).

Given the biological importance of the C-terminal region of Sir4 for establishing silent chromatin and many other potentially interesting protein-protein interactions, we have determined a crystal structure of this domain comprised by Sir4-C1 (residues 1198–1358) at 3.1 Å resolution. The C-terminal domain of Sir4 forms a parallel, two-stranded coiled coil with an unusual pairing of leucines at the **a** position of the heptad repeat and a variety of polar and nonpolar residues at the **d** position. Immediately N-terminal to the coiled coil is a poorly ordered segment that appears to be unfolded in solution. This unfolded segment might provide a flexible linkage between the coiled-coil protein interaction domain of Sir4 and the upstream region that binds to Sir2. We have identified the Sir3 binding site on the surface of the Sir4 coiled-coil domain by site-directed mutagenesis and show that one Sir3 dimer is bound to the dimeric coiled coil of Sir4. Furthermore, we have assembled in vitro a stable complex consisting of an N-terminally truncated Sir4 bound to both Sir2 and Sir3. These structural, biophysical, and genetic studies with model peptides and protein fragments have pinpointed specific interactions of the Sir proteins that will be helpful for dissecting their cellular roles in transcriptional silencing and in the maintenance of genomic stability.

Results and Discussion

Sir4 Dimerizes through a C-terminal Coiled-Coil Domain

We have determined a crystal structure of the protein interaction motif from the C terminus of the *Saccharomyces cerevisiae* Sir4 protein by multiple-wavelength anomalous-scattering methods using crystals of the selenomethionine-containing protein (Table 1). The Sir4-C1 peptide that was crystallized spans amino acids 1198–1358 of Sir4, encompassing an eleven-heptad hydrophobic repeat that was predicted to form a coiled coil (Figures 1A and 2A) (Gasser and Cockell, 2001). The experimentally phased electron density (Figure 1B) clearly revealed residues 1271–1346 of Sir4-C1 in the form of a continuous parallel coiled coil with another molecule. A 2-fold axis of crystallographic symmetry relates the subunits of the dimer (Figure 1B). The overall structure of the Sir4 fragment is typical of a coiled-coil dimer, with two extended α helices that pack together in a left-handed superhelix (Figure 1B). The N-terminal half of Sir4-C1 (residues 1198–1270) was not visible in any electron density maps using the experimental and/or model phases, calculated at different ranges of resolution. C-terminal residues 1347–1358 of the Sir4-C1 peptide are also disordered in the electron density. The Sir4-C1 peptide in the crystals was analyzed by SDS-PAGE and found to be intact and not degraded (data not shown). We conclude that the region immediately N-terminal to the coiled-coil domain of Sir4-C1 is either unstructured or forms an ensemble of structures that are statically disordered in the crystals. This flexible region of the Sir4 protein might play a role in regulating its interactions with Sir3 (Hoppe et al., 2002; Moazed et al., 1997), as discussed below.

Table 1. Data Collection, Phasing, and Refinement Statistics

Data Collection			
	Peak	Edge	Remote
Wavelength (Å)	0.97827	0.978423	0.95
Resolution (Å)	3.1	3.1	3.1
Total data	191,300	191,326	191,943
Unique data	4,796	4,796	4,793
Redundancy	11.20	11.22	11.21
Completeness (%)[a]	96.2 (97.2)	96.2 (97.2)	96.1 (97.3)
Mean I/σ[a]	33.3 (9.2)	30.5 (8.6)	31.0 (8.8)
R_{merge} (%)[a]	6.6 (30.3)	7.1 (33.5)	7.0 (33.5)
Phasing (SOLVE)			
Figure of merit	0.53		
Z score[b]	10.50		
Refinement			
Resolution (Å)	47.14–3.10		
R_{work}	0.271		
R_{test} (10% of all reflections)	0.288		
Mean B value (Å^2)	54.99		
Rms deviations			
Bond length (Å)	0.013		
Bond angle (°)	1.184		
Number of nonhydrogen atoms	573		

[a] Numbers in parentheses represent statistics in highest resolution shell (3.21–3.10 Å).
[b] See Terwilliger and Berendzen (1999) for the definition of the Z score.

Although its structure is typical of a coiled coil, the sequence of the Sir4 C-terminal domain is rather unusual. Coiled-coil proteins are characterized by a repeating pattern of seven residues, $(\mathbf{abcdefg})_n$, with hydrophobic amino acids predominating at positions **a** and **d** of the heptad repeat (Burkhard et al., 2001). The **a** and **d** positions define a stripe of residues along one side of an α helix that is buried by the packing together of two α-helical subunits. In the coiled coil, the side chains of residues **a** and **d** (the knobs) are inserted into spaces (the holes) between the side chains of the apposing α helix to create a "knobs into holes" packing of residues at the dimer interface (Crick, 1953). The superhelical twist of a coiled-coil dimer maintains the close contact between subunits over a greater area than

A

```
1191
YGYFSVGKRV PIVEDRRVKQ LDDITDSNTT EILTSVDVLG THSQTGTQQS

1241
NMYTSTQKTE LEIDNKDSVT ECSKDMKEDG LSFVDIVLSK AASALDEKEK
                                  abcdefgabc defgabcdef

1291
QLAVANEIIR SLSDEVMRNE IRITSLQGDL TFTKKCLENA RSQISEKDAK
gabcdefgab cdefgabcde fgabcdefga bcdefgabcd efgabcdefg

1341
INKLMEKDFQ VNKEIKPY
abcdefg
```

B

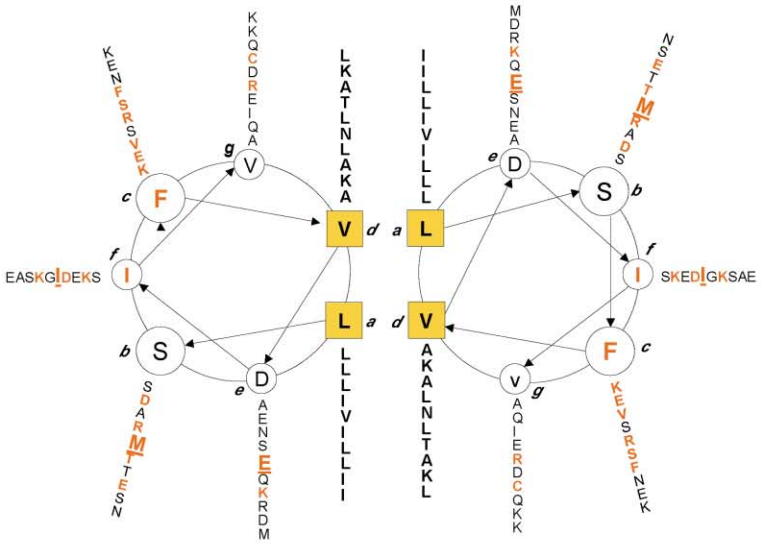

C

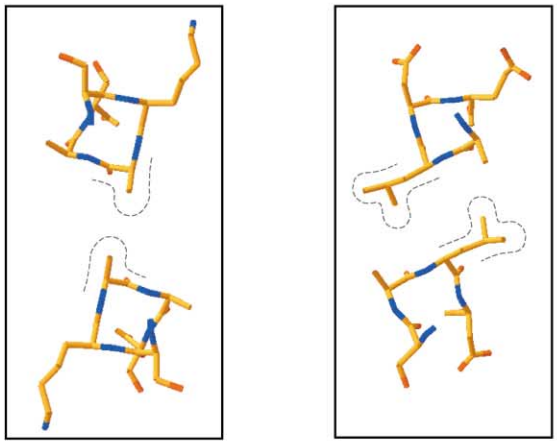

Figure 2. Heptad Repeat and Packing of Interfacial Residues of the Sir4 Dimer

(A) The residues of the 11-heptad repeat of the Sir4 coiled coil, assigned according to the crystal structure, are displayed in red below the sequence of the C-terminal region of Sir4. Six leucines in the heptad repeat of the coiled coil are located in the **a** position of the heptad repeat, instead of in the **d** position as is commonly observed for leucines in leucine zipper-type coiled coils. The **d** positions of the heptad are occupied by a variety of polar and nonpolar residues.

would be possible with straight α helices. α helices can also pack together in compact bundles consisting of three or more α helices.

The oligomeric state of a bundle of α helices is strongly influenced by the shapes of the nonpolar side chains at the **a** and **d** positions of the constituent helices and, in particular, the abundance of β-branched residues like isoleucine or valine at the **a** position (Harbury et al., 1993, 1994). In parallel coiled-coil dimers, the **a** position is unusually enriched for β-branched residues, whereas the **d** positions are depleted of β-branched residues and leucine is often prominently featured at this position. These preferences for β-branched and unbranched side chains at the **a** and **d** positions, respectively, reflect two different modes of side chain interactions across the dimerization interface (Figure 2C). The side chains of residue pairs at the **a** position pack with their Cα-Cβ bonds aligned in a parallel orientation and their side chains extending toward opposite sides of the dimer (Figure 2C, right panel). The β-methyl groups of isoleucine or valine side chains are readily accommodated by this parallel packing. The perpendicular packing at position **d** instead points the Cα-Cβ bonds of interacting residues toward the dimer interface (Figure 2C), resulting in less space for the β-methyl group of isoleucine or valine. Higher-order α-helical bundles consisting of three or more helices show different amino acid preferences that reflect a more extensive buried core of residues. In four-helix bundles, the residue preferences at the **a** and **d** positions are reversed, with the **a** positions favoring leucine and the **d** positions favoring β-branched side chains. (Harbury et al., 1993, 1994). Three-helix bundles show little bias for particular amino acid types at either the **a** or **d** position.

Although the Sir4 coiled coil exhibits the usual knobs into holes packing, its amino acid sequence does not conform to the consensus for coiled-coil dimers. The leucine heptad repeat of Sir4 populates the **a** position of the coiled coil (Figure 2A), instead of the **d** position as is characteristic of leucine zipper-style coiled coils (Alber, 1992). Six of 11 **a** position residues are leucine, and the remaining **a** residues comprise four isoleucines and a valine (Figure 2B). There is no obvious consensus residue in the **d** position of Sir4, which is populated by seven nonpolar residues and four polar residues spaced throughout the length of the coiled-coil sequence. The polar residues K1288, N1309, T1323, and K1337 in the **a** position make close van der Waals packing interactions with their dimerization partners using the aliphatic carbons of their side chains. The polar atoms of the side chains from K1288, T1323, and K1337 point away from the dimer interface and toward solvent. However, N1309 is oriented so that it could hydrogen bond with N1309′ of the apposing subunit, similar to the interaction of N264 in the **a** position of the GCN4 leucine zipper dimerization motif (O'Shea et al., 1991). This interaction would violate the crystallographic 2-fold symmetry axis relating the two subunits of Sir4, but it is accommodated by two alternative orientations of the N1309 side chain in the crystallographic model. Although polar residues at the **a** or **d** positions can decrease the stability of coiled-coil dimers, a hydrogen bonding interaction like that proposed for N1309 may serve to align subunits of the dimer in the proper register (Akey et al., 2001; Burkhard et al., 2000).

Much of the dimerization energy of a coiled coil derives from van der Waals packing interactions between the buried, nonpolar residues located at the **a** and **d** positions (Alber, 1992; Arndt et al., 2002; Kohn et al., 1997). Salt bridges and hydrogen bonds between the residues flanking the dimerization interface (positions **e** and **g**; Figure 2B) can provide additional stability to coiled-coil dimers (Marti et al., 2000). Both of the **d** position lysines noted above interact with acidic residues in the nearby **e** position of the apposing Sir4 subunit. Lysine 1288 (**d**) bonds to E1289′ (**e**) of the opposite subunit, and K1337 (**d**) engages D1338′ (**e**). In addition, R1312 (**g**) is hydrogen bonded to Q1317′ (**e**).

The abundance of polar residues at position **a** of the Sir4 subunit interface and the paucity of other stabilizing interactions might adversely affect the stability of the Sir4 dimer. The resulting monomer-dimer equilibrium of Sir4 could in turn affect its interactions with other Sir proteins during the establishment of silenced chromatin (Hoppe et al., 2002). To address whether the atypical sequence of Sir4 translates into weaker dimerization of its coiled coil, we used circular dichroism (CD) spectroscopy and analytical ultracentrifugation to monitor the folding and dimerization of the Sir4-C1 peptide. The CD spectrum of Sir4-C1 is characteristic of an α-helical protein (Figure 3). At a protein concentration of 2.5 μM Sir4-C1 monomer, the thermal denaturation of the peptide reveals a sharp transition from folded dimer to unfolded monomers, with a melting temperature (Tm) of 33°C (Figure 3A). The folded Sir4-C1 peptide is 44% α helical, judging from the deconvolution of its CD spectrum collected at 4°C, corresponding to about 70 residues in an α-helical conformation (Table 2). This observation is in good agreement with the number of residues visible in the crystal structure of the Sir4-C1 coiled coil (Figure 2) and suggests that the coiled-coil region is completely folded at low micromolar concentrations of the monomer. The CD spectrum of a shorter Sir4-C2 peptide spanning only the coiled-coil region of Sir4-C1 (Figure 1) has a similar value at 222 nM to the longer Sir4-C1 peptide (Figure 3B). Deconvolution of the CD spectrum of Sir4-C2 again reveals about 70 residues in an α-helical conformation (Table 2). These results con-

(B) A helical wheel representation of the repeated sequence of the Sir4 coiled coil highlighting the **a** and **d** positions at the center of the dimer interface. The positions of the heptad repeat are labeled ***a–g***. Solvent-exposed residues that were mutated to identify the binding site for Sir3 (cf. Figure 5) are shown in red, and the residues that are required for binding to Sir3 are shown underlined and in bold red.

(C) Side chains at the **d** position of the coiled-coil heptad (left panel) pack together across the dimer interface in a perpendicular packing arrangement that disfavors the β-methyl group of valine or isoleucine side chains. Residues in the **a** position pack in a parallel arrangement that makes room for β-branched residues. Unlike most dimeric coiled coils, non-β-branched leucine residues predominate in the **a** position of the Sir4 coiled coil.

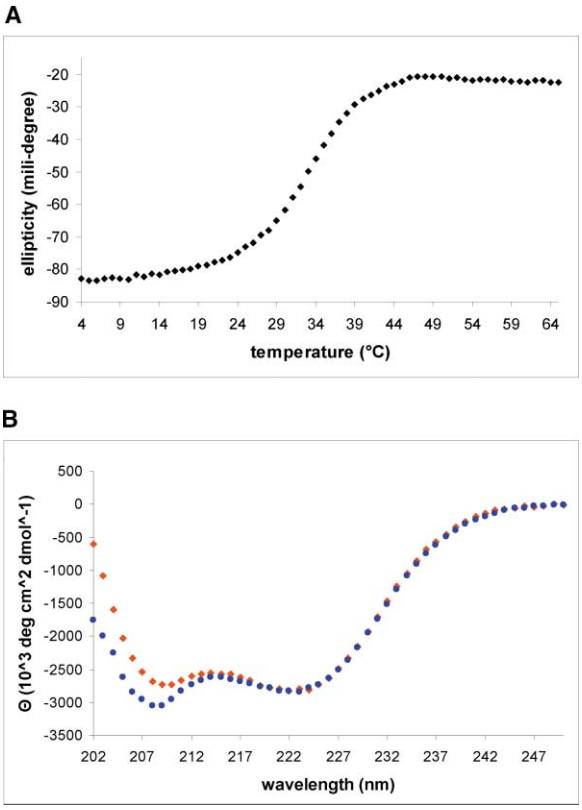

Figure 3. The Sir4 Coiled Coil Is Abutted by an N-Terminal Unstructured Region

(A) The thermal unfolding of Sir4-C1 was monitored from the change in elipticity of the peptide at 222 nm. The data show a single melting transition centered at 33°C, indicating that Sir4-C1 is a stable dimer at a concentration of 2.5 μM and shows no evidence of higher-order oligomers.

(B) The CD spectra of the Sir4-C1 (blue circles) and the shorter Sir4-C2 peptide (red diamonds), which spans only the ordered region in the crystal structure (cf. Figure 1), reveal a similar number of residues in an α-helical conformation (see text for analysis of the spectra). However, the divergence of the spectra in the far-UV region is consistent with the additional residues of the Sir4-C1 peptide forming a random coil. The comparison of the Sir4-C1 peptide that was crystallized with the Sir4-C2 coiled-coil peptide shows that the N-terminal region of Sir4-C1 is disordered in solution.

firm the N-terminal 74 residues of the Sir4-C1 peptide that was crystallized do not contribute to its CD spectrum and are probably unfolded in solution. The shorter Sir4-C2 peptide is significantly less soluble than Sir4-C1, and some precipitate formed during the lengthy thermal melting studies. It was therefore difficult to directly compare the stability of the Sir4-C2 dimer with that of the Sir4-C1 dimer. Although both proteins have a similar α-helical content, the N-terminal extension of Sir4-C1 dramatically improves solubility. These results suggest that residues 1198–1270 of Sir4 serve as a loosely structured, flexible link between the C-terminal coiled-coil dimerization motif and the N-terminal region that includes the binding site for Sir2. In support of this notion, this region is susceptible to proteolytic degradation as discussed below.

The Sir4-C1 protein elutes from a gel filtration column as a single species, yet the estimated molecular weight relative to globular protein standards is about 1.5-fold larger than the calculated mass of the Sir4-C1 dimer. The rod-like shape of the coiled coil as well as the appended unstructured region of Sir4-C1 could affect this molecular weight estimate. We therefore used the technique of equilibrium sedimentation to estimate the native size of the Sir4-C1 peptide (Table 3). The results obtained with several different concentrations of Sir4-C1 all agree with the expected size of the Sir4-C1 dimer. Despite the atypical amino acid sequence of the Sir4 coiled coil, it is a stably folded dimer at micromolar protein concentrations.

Sir3 Binds to a Hydrophobic Patch on the Surface of the Sir4 Coiled Coil

The C-terminal region of Sir4 encompassed by Sir4-C1 (residues 1198–1358) interacts with a number of different protein factors involved in transcriptional regulation and DNA silencing (Cockell et al., 1995; Moazed and Johnson, 1996; Moretti and Shore, 2001; Tsukamoto et al., 1997), including a direct physical interaction of Sir3 (Moazed et al., 1997; Moretti et al., 1994). We undertook a mutational analysis of Sir4-C1 to identify the binding site for Sir3 using the crystal structure as a guide. In particular, we wished to determine whether Sir3 binds to the disordered N-terminal region of Sir4-C1 or to the coiled coil. Binding to either site could have different implications for the stoichiometry of the Sir4-Sir3 complex and the Sir4 monomer-dimer equilibrium.

We initially investigated the interaction of Sir3 with a series of N-terminally truncated fragments of Sir4 fused to glutathione-S-transferase (GST) using a pull-down assay with glutathione Sepharose beads. Using a series of Sir4 fragments with N termini located between amino acids 1198 and 1267 (upstream of the coiled coil) and extending to the authentic C terminus of Sir4 (residue 1358), we measured interactions with Sir3 (residues 1–978) purified from yeast or with a C-terminal fragment of Sir3 (Sir3T; residues 464–978) purified from an overexpressing strain of *Escherichia coli*. The Sir3T protein encompasses the regions of Sir3 that interact with Sir4 and with the N-terminal tails of histones (Hecht et al., 1995; Moazed et al., 1997; Moretti et al., 1994; Park et al., 1998). We were surprised to find that the coiled-coil domain of Sir4 (the Sir4C-2 peptide; Figure 1A) is by itself sufficient for a stable interaction with Sir3 or Sir3T, forming complexes that survive extensive washing (Fig-

Table 2. Secondary Structure from CD Spectra Decomposition

	R Factor (%)	α Helices (%)	β Strands (%)	Others (%)	Total Number of Residues	Number of Residues in α Conformation
Sir4-C1	4.55	44.15	14.00	41.85	161	71
Sir4-C2	4.71	76.45	5.96	17.59	92	70

Table 3. Molecular Weight Determination with Equilibrium Sedimentation

Protein	Concentration (μM)	Estimated MW (KDa)	Monomer MW (KDa)	$MW_{estimated}/MW_{monomer}$
Sir4-C1	150	38.1	18.2	2.1
	83	37.1	18.2	2.0
Sir3T	12.5	109.0	60.3	1.8
	6.3	143.1	60.3	2.4

ure 4). The Sir4-C2 coiled coil binds as efficiently as Sir4-C1, indicating that the upstream disordered region of Sir4-C1 does not significantly contribute to the interaction with Sir3. We conclude that, in addition to dimerizing Sir4, the C-terminal coiled-coil domain contains the binding site for the Sir3 protein.

Based on the crystal structure of Sir4-C1, a series of point mutants were generated with amino acids substituted on the surface of the coiled coil in order to identify the binding site for Sir3. Initially, eleven mutations were designed that spanned the length of the Sir4-C2 coiled coil at exposed positions that should not interfere with dimerization. The mutant proteins were overexpressed in *E. coli* as GST fusions for pull-down assays with Sir3T. Most of the mutant Sir4 peptides bound to Sir3T about as efficiently as wild-type Sir4-C2 (Figure 5A). The K1324E and K1325E mutants showed a slight and variable decrease in binding efficiency in several independent experiments (Figure 5A). However, the I1311N mutant consistently failed to interact with Sir3 (Figure 5A). Ten more mutant Sir4 proteins were prepared with substitutions of surface residues around I1311. The M1307N mutation prevented binding to Sir3, whereas the E1310R mutation strongly interfered with Sir3 binding (Figure 5A). As a control, we confirmed by CD spectroscopy that the I1311N, M1307N, and E1310R mutant peptides without the GST affinity tag are well-folded α helices, like the wild-type Sir4 coiled coil (data not shown). The residues that are critical for binding to Sir3 are clustered together near the middle of the Sir4 coiled coil, forming two predominantly hydrophobic patches on both subunits of the dimer (Figures 1B and 5B). Although the Sir3 interaction surface might extend outside of these small patches of residues, amino acid substitutions at many of the surrounding residue positions had no effect on Sir3 binding in the pull-down assay (Figure 5A). These experiments show that the coiled-coil domain of Sir4 interacts directly and specifically with Sir3. Given the stability of the Sir4 coiled-coil dimer and the presence of two identical binding sites for Sir3, it seemed likely that Sir3 and Sir4 would interact in a 2:2 complex (Figure 5B). This binding stoichiometry could facilitate polyvalent interactions with other proteins during the establishment and spreading of silenced DNA.

The region of Sir3 that interacts with Sir4 was previously localized to a fragment of Sir3 spanning residues 482–835 (Moazed et al., 1997). In order to more precisely define the Sir3 side of the Sir3-Sir4 interface, a series of N-terminally truncated Sir3 fragments were tested for binding to GST-Sir4-C2 (Figure 5C). Whereas a C-terminal fragment of Sir3 starting at residue 495 binds efficiently to Sir4-C1, larger N-terminal deletions extending beyond residue 510 fail to interact with Sir4 (Figures 5C and 5D). Therefore, the region of Sir3 spanning residues 495–521 is particularly crucial for interactions with Sir4. Secondary structure predictions based on the amino acid sequence of Sir3 suggest that residues 505–516 could adopt an α-helical conformation. However, we observed that the N-terminal region of the Sir3T protein is susceptible to proteolytic degradation. Digestion of Sir3T with elastase, trypsin, or chymotrypsin produces a fragment with an apparent molecular weight of ~50 kDa (estimated by SDS-PAGE) that is resistant to further degradation. A Western blot of these digestion products confirmed that all three enzymes cleave at the N terminus of Sir3T while leaving intact a C-terminal His_6 affinity

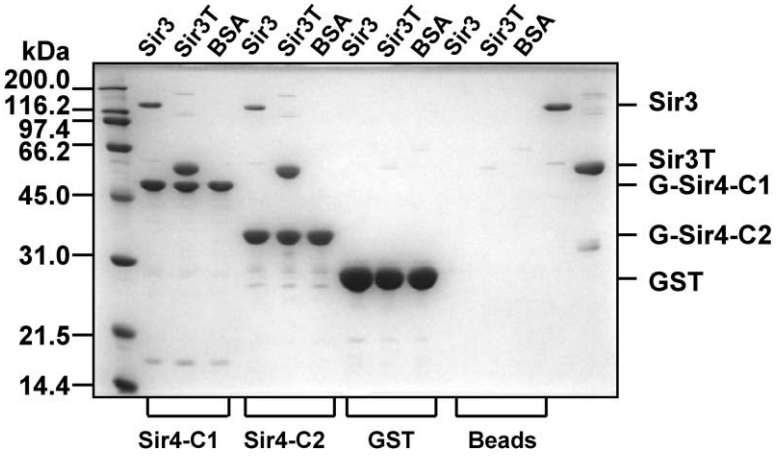

Figure 4. The Coiled-Coil Domain of Sir4 Physically Interacts with Sir3

The association of the C-terminal domain of Sir4 with full-length Sir3 and the Sir3T fragment (residues 464–978) was assayed by pull-down experiments. The GST-tagged Sir4-C1 or Sir4-C2 proteins (cf. Figure 1) were bound to glutathione Sepharose and then incubated at 4°C with Sir3, Sir3T, or BSA as a control. Proteins complexed to the beads were run on an SDS-PAGE gel and stained with Coomassie blue. The purified Sir3 and Sir3T proteins used for the pull-down experiments are shown in the rightmost two lanes of the gel. Sir3 and Sir3T both bind efficiently to Sir4-C1 and Sir4-C2, whereas they do not associate with the GST protein or glutathione Sepharose beads lacking Sir4. The smaller amount of Sir3 in comparison to Sir3T in the complexes results from less Sir3 used in the initial binding reaction. The coiled-coil domain alone, represented here by Sir4-C2, is sufficient by itself for interactions with Sir3.

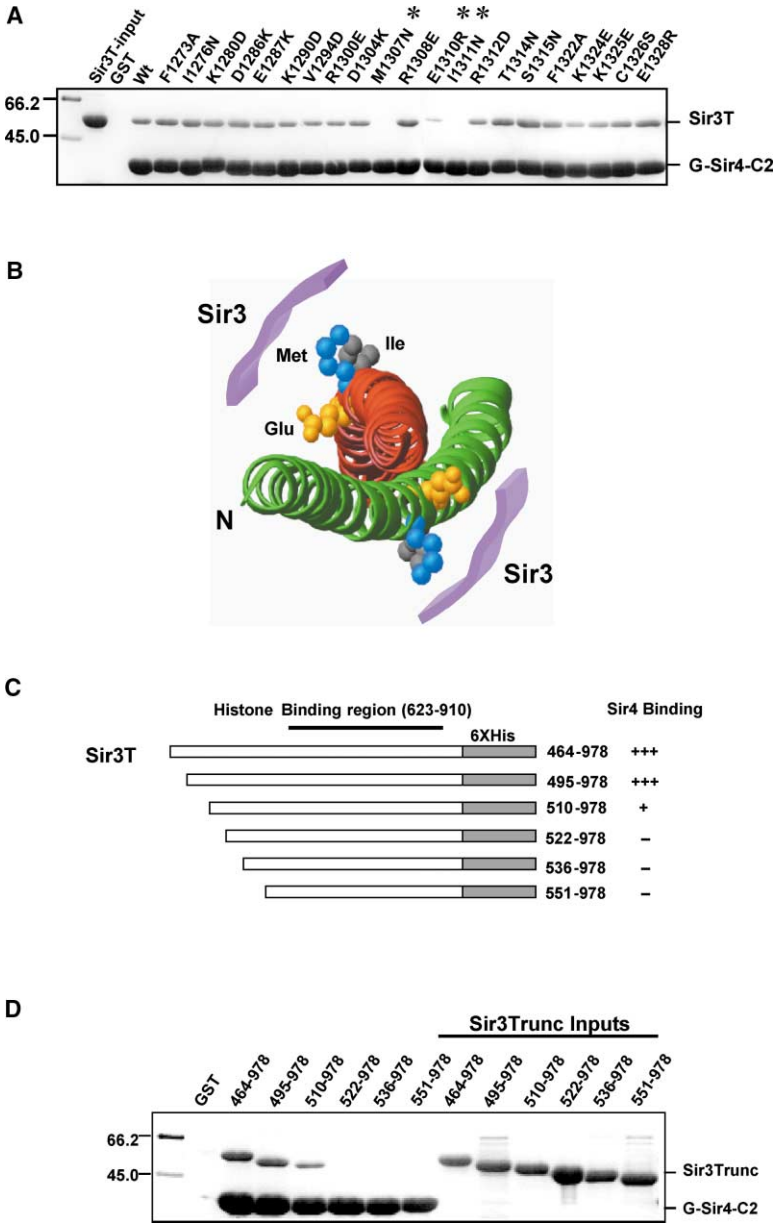

Figure 5. A Hydrophobic Patch of Residues on the Surface of the Sir4 Coiled Coil Binds Sir3

(A) A series of mutant Sir4-C2 proteins with amino acid substitutions at the exposed positions along the length of the coiled coil were constructed and tested for interaction with Sir3T by the GST pull-down assay with a 1:1 molar ratio of Sir3T and each Sir4-C2 mutant. Mutation of residues M1307 and I1311 prevent binding to Sir3T, and mutation of the neighboring residue E1310 strongly interferes with binding to Sir3T.

(B) The locations of the Sir4 residues that are required for interaction with Sir3 are shown, colored as in Figure 1B. The Sir3 binding site is present on each subunit of the coiled-coil dimer, suggesting that two Sir3 molecules interact with the Sir4 dimer (cf. Figure 6).

(C) A series of N-terminally truncated Sir3 proteins were tested for interaction with the GST-Sir4-C2 coiled-coil domain. The Sir3 proteins were expressed in *E. coli* and purified with a C-terminal His_6 affinity tag prior to use in the pull-down experiment. The efficiency of the interaction with Sir4-C2 is shown.

(D) Pull-down assays are shown that test the interaction of Sir4 with a series of N-terminally truncated Sir3 proteins. The results show that the region of Sir3 between residues 495 and 522 is crucial for efficient binding to Sir4. This region is exposed and proteolytically sensitive in the absence of Sir4 (see text for details).

tag. Amino acid sequencing shows that elastase cleaves Sir3 after residue 527. These findings suggest the critical residues at the N terminus of Sir3T that are required for its interactions with Sir4 are exposed and susceptible to proteolysis in the absence of the Sir4 protein.

A Sir3 Dimer Binds to the Coiled Coil of Sir4

The Sir4 coiled coil is a stable dimer that binds to Sir3 (Table 3). The native state of the Sir3T protein was similarly analyzed by gel filtration and by sedimentation equilibrium experiments. Sir3T elutes as a single species from a gel filtration column with an apparent molecular weight of about 120 kDa (data not shown), or roughly twice the size predicted for the 516-residue Sir3T monomer. Sedimentation equilibrium experiments confirmed that native Sir3T is a dimer (Table 3).

Because of the potential complexities associated with fitting the data for an interaction involving two multimeric proteins, together with the vastly different sizes of the Sir4-C1 dimer and the Sir3 dimer, we decided to investigate the Sir4-Sir3 complex by another method. Isothermal titration calorimetry (ITC) was used to measure the molar stoichiometry of Sir4 and Sir3 proteins in the complex. The Sir4-C1 peptide (200 μM stock) was injected into a reaction cell containing Sir3T (25 μM). The interaction of Sir4 with Sir3 is strongly endothermic when measured at an ambient temperature of 10°C (Figure 6A). In contrast, a control experiment in which Sir4-C1 was injected in the absence of the Sir3 protein generates only small exothermic peaks that correspond to the dilution heat of the Sir4 protein. The magnitude of the dilution heat of Sir4-C1 is very similar to the peaks observed at the end of the titration experiment when Sir3 binding is saturated. Under conditions of excess Sir4-C1, the

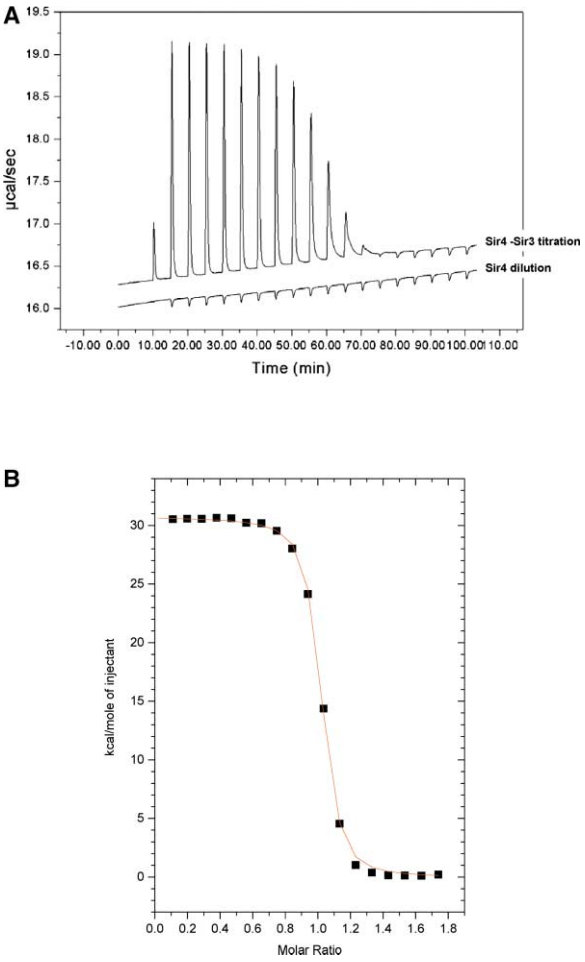

Figure 6. The Sir4 Coiled Coil Forms a 1:1 Complex with Sir3T

(A) The raw isothermal titration calorimetry data are shown for a titration of Sir4-C1 into buffer containing Sir3T (top trace) or into the reaction buffer alone (bottom trace). The binding reaction at 10°C is endothermic and saturable. The injection of excess Sir4-C1 at the end of the titration generates a signal that is very similar to the dilution of Sir4-C1 alone.

(B) The integrated heats are shown as a function of molar ratio of Sir4-C1 to Sir3T, after correction for the heats of dilution and injection. The binding interaction is strongly endothermic (30.7 kcal mol^{-1}) and saturates at a 1:1 molar ratio of Sir4-C1 and Sir3T. Given that Sir3T and Sir4-C1 separately are stable dimers (see text for details), we propose that one Sir4 dimer associates with one Sir3 dimer in the native complex.

addition of more Sir4-C1 generates only a dilution signal (Figure 6A). In Figure 6B the integrated heats of binding (after correction for the heats of dilution and injection) are plotted as a function of the molar ratio of Sir4-C1 to Sir3T. The ITC binding data indicate that the complex consists of a 1:1 molar ratio of Sir4-C1 and Sir3T. Gel filtration of the complex of Sir4-C1 with Sir3T yields a unique peak that elutes at an apparent molecular weight of about 260 kDa (data not shown). Compared with the elution positions of the Sir4-C1 dimer (~60 kDa) and the Sir3T dimer (~120 kDa) run separately, the complex of Sir4-C1 and Sir3T is likely to contain two to three molecules of each protein. Since both Sir4-C1 and Sir3T are stable dimers in solution (Table 3), it is likely that the native complex of the full-length proteins consists of one Sir4 dimer bound to a Sir3 dimer. Although we were unable to measure an accurate binding constant for the Sir4-Sir3 interaction because of the high protein concentrations used in ITC, other experiments, including the pull-down assays and gel filtration of the complex, suggest that these proteins are tightly associated in the complex. The binding of Sir3 to histone tails has been previously reported (Carmen et al., 2002; Hecht et al., 1995; Hoppe et al., 2002), but we were unable to detect a stable interaction of Sir3T with GST-fused histone tail peptides that were immobilized on agarose beads (data not shown). The stable interaction of Sir3 with chromatin may require additional interactions with the DNA-bound Sir4-Sir2 complex.

The purified Sir3T protein has a tendency to aggregate at physiological temperatures (20°C–30°C), and it slowly precipitates at the protein concentrations required for ITC. The binding experiments were therefore performed at 10°C. At this temperature the binding of Sir4-C1 to Sir3 is an endothermic reaction (Figure 6) with a large positive enthalpy change of about 30.7 kcal mol^{-1}. Although the enthalpy change could not be accurately measured at higher temperatures because of Sir3T's tendency to precipitate, the binding of Sir4-C1 to Sir3T is an exothermic reaction at 20°C, with a relatively small enthalpy change (−8.3 kcal mol^{-1}; data not shown). This suggests that the enthalpy change associated with protein complex formation is strongly temperature dependent. In other words, the binding of Sir4 to Sir3 is associated with a large and negative change in heat capacity. This is the thermodynamic signature of a binding reaction that is coupled to the folding of a protein or some other event resulting in the burial of an unusually large amount of exposed surface area in the complex (Jelesarov and Bosshard, 1999; Ladbury and Chowdhry, 1996; Leavitt and Freire, 2001). At least two factors could contribute to the large and negative change in heat capacity associated with the complexation of Sir4 and Sir3. First, the solvent-exposed surfaces of Sir3 and Sir4 that are buried in the complex may be unusually hydrophobic. This idea is consistent with the tendency of Sir3T to aggregate prior to binding to Sir4-C1 and with the hydrophobic patch on Sir4 that binds to Sir3 (Figure 5B). Secondly, the proteolytically sensitive N-terminal region of Sir3T (residues 495–527) might become stably folded upon binding to Sir4.

Assembly of a Ternary Complex of Sir2/Sir4/Sir3

Sir3 is important for the spreading and maintenance of silent DNA (Hecht et al., 1996; Hoppe et al., 2002; Moretti et al., 1994). However, native Sir4-Sir2 complexes isolated from yeast lack the Sir3 protein (Ghidelli et al., 2001; Hoppe et al., 2002; Moazed et al., 1997), despite significant amounts of free Sir3 in yeast cells. These findings suggest that the interaction of Sir3 with Sir4-Sir2 might be regulated by, or dependent on, interactions with chromatin. It is possible that the flexible unstructured region immediately upstream of Sir4's coiled coil could aid in sequestering the binding site for Sir3. To test this idea, we prepared the 613-residue Sir4-C3 protein that spans the binding sites for both Sir2 and Sir3

(Figure 1A). Sir4-C3 is sparingly soluble, and it copurified with a 70 kDa molecular chaperone, as previously reported (Figure 7A, lane 5) (Hoppe et al., 2002; Moazed et al., 1997). After incubation of GST-Sir4-C3 with a molar excess of either Sir2 (Figure 7A, lane 3) or Sir3T (lane 4), binary complexes of these proteins can be affinity purified with glutathione agarose beads. In control experiments Sir2 and Sir3T did not bind to GST-agarose beads or to glutathione-S-transferase protein immobilized on the beads (data not shown). On the basis of the Coomassie staining intensities of the proteins in these complexes, it appears that not all of the Sir4-C3 protein is available for interaction with Sir2 or Sir3T, perhaps because of aggregation of Sir4-C3 or interference by the chaperone protein that copurified with Sir4-C3. Despite this limitation of our assay, it is evident that the binding sites for Sir2 and for Sir3T are accessible in the longer Sir4-C3 protein.

We next asked whether Sir3 can bind to Sir4-C3 in complex with Sir2. The Sir4-C3 protein (Figure 1A) was immobilized on glutathione agarose beads and preincubated with a 25-fold molar excess of Sir2 to saturate binding before exchanging the beads into a 10-fold molar excess of Sir3T (Figure 7A, lane 6). Sir3T binds as efficiently to a complex of Sir4-C3 with Sir2 as it does to Sir4-C3 alone (Figure 7A, compare lanes 4 and 6). The lack of competition shows that Sir2 and Sir3 bind independently to Sir4-C3. We confirmed that Sir3T binds specifically in the ternary complex of Sir2/Sir4/Sir3 by repeating the pull-down experiment using a point mutant designed to block the interaction of Sir3 with the coiled-coil domain of Sir4-C3 (the I1311N mutation; Figure 5A). The I1311N mutant Sir4-C3 protein fails to interact with Sir3T, whereas this mutation does not affect binding by Sir2 (Figure 7B, compare lanes 3 and 6). It is also noteworthy that Sir2 does not rescue the interaction of Sir3T with the Sir4 I1311N mutant, giving no evidence for a cooperative interaction of Sir2 and Sir3 in the complex. We conclude that the binding sites for Sir2 and Sir3 function independently and are well separated in the Sir4 protein.

Biological Implications

Transcriptional silencing through the formation of silent chromatin in budding yeast is a highly regulated, stepwise process that involves the assembly of the silent information regulators Sir2, Sir3, and Sir4 into a multiprotein complex (Gasser and Cockell, 2001; Hecht et al., 1995; Hoppe et al., 2002; Luo et al., 2002; Moazed, 2001; Rusche et al., 2002; Wyrick et al., 1999). Silencing is initiated by the transient recruitment of the Sir2-Sir4 complex to DNA. The formation of this initial complex does not require the deacetylase activity of Sir2 and is independent of Sir3. However, Sir3 is required for the stabilization and spreading of silent chromatin. In contrast to Sir2 and Sir4, which form a constitutive complex in vivo, the interaction of Sir3 and Sir4 appears to be less stable and may be subject to regulation. Sir3 interacts with Sir4 and with deacetylated histone tails (Carmen et al., 2002; Hecht et al., 1995; Hoppe et al., 2002). The Sir3-Sir4 interaction is important for the localization of Sir3 at silencers and the propagation of silent chromatin (Hoppe et al., 2002).

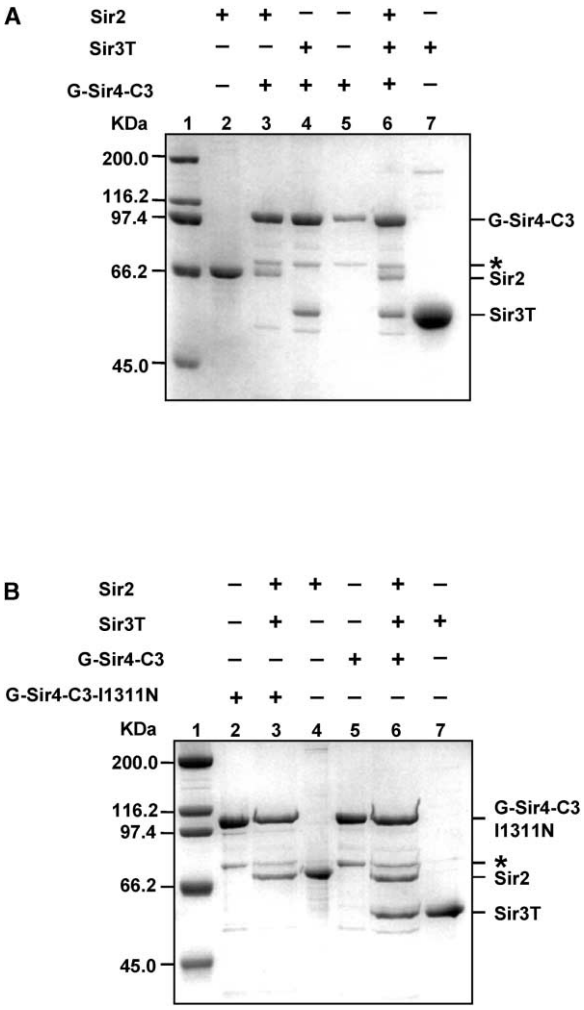

Figure 7. Sir4 Forms a Ternary Complex with Sir2 and Sir3

(A) The interaction of GST-Sir4-C3 (residues 745–1358; cf. Figure 1) with Sir2 and Sir3T was assayed by pull-down experiments. A Comassie blue-stained SDS-PAGE gel of the protein complexes and several standards is shown. Sir4-C3 (lane 5) copurifies with the molecular chaperone *E. coli* DnaK (labeled with an asterisk) as well as several putative breakdown products of Sir4. Sir4-C3 binds specifically to Sir2 (lane 3) or to Sir3T (lane 4). On the basis of Comassie staining intensity, it appears that not all the Sir4-C3 in the binding reaction is capable of binding to Sir2 or Sir3, perhaps because of interference from DnaK and/or aggregation of Sir4-C3. Nonetheless, Sir2 and Sir3T incubated together bind to Sir4-C3 as efficiently (lane 6) as either protein separately (compare to lanes 3 and 4). This suggests that Sir2 and Sir3T bind to Sir4 independently and simultaneously.

(B) The pull-down experiments were repeated, but a 25-fold molar excess of Sir2 was preincubated with GST-Sir4-C3 (lanes 6) or the mutant protein GST-Sir4-C3 I1311N (lanes 3) before adding Sir3T. Sir3T still binds to Sir4-C3 in the presence of a vast excess of Sir2 (lane 6), indicating that binding of Sir2 does not interfere with binding of Sir3. The I1311N mutant of Sir4 disrupts the interaction with Sir3 (cf. Figure 5A) and selectively interferes with Sir3 binding in the ternary complex, as well (lane 3). The formation of a ternary Sir2/Sir3/Sir4 complex highlights the importance of the Sir3-Sir4 interaction for recruiting Sir3 to silencers and the subsequent spreading of silent chromatin through the action of the Sir2 deacetylase and Sir3's dual interactions with Sir4 and hypoacetylated histones.

Here we demonstrate a stable association of Sir3 with Sir4 in vitro using truncated protein constructs and identify specific regions of both proteins that are required for this interaction. Our crystallographic and biochemical data show that the extreme C terminus of Sir4 is a dimeric coiled coil that binds directly to a Sir3 dimer in a discrete 1:1 molar ratio. The stable interaction of Sir3 with Sir4 is mediated by a hotspot of hydrophobic residues located on the surface of each subunit of the coiled-coil dimer. The strength and specificity of this protein-protein interaction suggest that it is of primary importance for recruiting Sir3 to silencers. Our results also indicate that the interaction of Sir4 with Sir3 is accompanied by a conformational change in both proteins. The Sir4 residues immediately N-terminal to the coiled coil (residues 1198–1270) are disordered in the crystal structure and these residues are also susceptible to proteolytic degradation in the larger Sir4-C3 protein. We propose this segment is an unstructured, flexible linker of Sir4 that joins the coiled-coil binding site for Sir3 to the upstream region that interacts with Sir2. Additionally, we have identified a small region of Sir3 (residues 495–522) that is essential for binding to the Sir4 coiled coil. This interaction surface is susceptible to proteolysis in the absence of Sir4, but it may become structured in the complex. Sir3 also interacts with deacetylated histones and it remains to be determined whether these interactions occur simultaneously with binding to Sir4. The association of Sir3 and Sir4 in a discrete complex consisting of a dimer of dimers places constraints on models for the formation of silent chromatin by polyvalent interactions of the Sir proteins.

Experimental Procedures

Preparation of Proteins

The Sir4-C1, Sir4-C2, Sir4-C3, and Sir4 fragments were expressed as glutathione-S-transferase (GST) fusion proteins and purified as previously described (Moazed et al., 1997). The thrombin cleavage site for removal of the GST affinity tag was replaced by a cleavage site for the PreScission protease (Amersham Biosciences). After proteolytic cleavage, the untagged Sir4 proteins were further purified by gel filtration on a Zorbax GF-250XL HPLC column (Dupont) as a final step. For production of selenomethionine (SeMet)-containing protein, the Sir4-C1 expression strain was grown in a defined medium containing selenomethionine and a cocktail of amino acids that represses methionine biosynthesis (Van Duyne et al., 1993). The SeMet protein was purified by following the same protocol as the native protein, except that 10 mM DTT was included in all buffers. Site-directed mutagenesis of GST-Sir4-C2 was performed with the QuickChange mutagenesis kit (Stratagene). The Sir4 mutants were purified by glutathione affinity chromatography before use in pull-down assays.

The genes for N-terminally truncated Sir3 proteins were cloned with C-terminal His_6 affinity tags in the pET24a vector (Novagen) between the NheI and NotI restriction sites. These Sir3 proteins were expressed in *E. coli* and purified in buffer containing 50 mM HEPES (pH 8.0), 500 mM KCl, 1 mM BME, and 5% glycerol with TALON metal affinity resin (Clontech). The proteins were eluted from the TALON column with buffer containing 200 mM imidazole. The full-length Sir3 protein was purified from a yeast strain that overexpresses a C-terminally TAP-tagged version of the protein under control of the GAL1 promoter (J.C.T and D.M., unpublished data). The gene encoding full-length Sir2 was cloned with an N-terminal His_6 affinity tag in the pET28 vector (Novagen) between the NdeI and XhoI restriction sites. The purification strategy for Sir2 was similar to that used for Sir3T.

Crystallization and Structure Determination

Purified Sir4-C1 was concentrated by ultrafiltration (Centricon 3; Amicon) to approximately 5 mg ml^{-1} in a buffer consisting of 50 mM HEPES (pH 7.5), 350 mM NaCl, 5 mM DTT, and 1 mM EDTA. Crystals of Sir4-C1 were grown at 22°C by the hanging drop vapor diffusion method from a 1:1 mixture of the protein with a well solution consisting of 100 mM MES (pH 6.0), 200 mM $MgCl_2$, and 1% PEG-3350. Crystals of native and SeMet Sir4-C1 are typically grow to dimensions of 150 μm × 150 μm × 100 μm, and they diffract X-rays to 3.5 Å resolution with a rotating anode X-ray source and to 3.1 Å resolution with synchrotron radiation. The crystals belong to the hexagonal space group $P6_522$ and have unit cell parameters of a = 108.64 Å, b = 108.64 Å, and c = 74.75 Å. One molecule of Sir4-C1 occupies the crystallographic asymmetric unit, corresponding to a V_M of 3.2 $Å^3$ Da^{-1}. A crystallographic 2-fold rotation axis relates the two subunits of the Sir4-C1 coiled-coil dimer in the crystal. A Wilson plot of the diffraction intensities for acentric reflections suggests that the crystals are not twinned. Multiwavelength anomalous diffraction (MAD) X-ray data were collected at beamline X-12C of the National Synchrotron Light Source (Upton, NY) and processed with the HKL2000 program suite (Table 1) (Otwinowski and Minor, 1997). The program SOLVE (Terwilliger and Berendzen, 1999) identified two sites of selenomethionine substitution in the crystals and, after heavy-atom parameter refinement in SOLVE, these phases produced interpretable electron density that was somewhat improved by solvent flattening with DM (Cowtan and Main, 1996) in the CCP4 suite of programs (Bailey, 1994). The crystallographic model was built with the program O (Jones et al., 1991) using the sites of selenium substitution to confirm the register of the amino acid sequence in the electron density. The model was refined with CNS (Brunger et al., 1998) and then by REFMAC (Murshudov et al., 1997) to an R_{free} of 28.8 % (Table 1). The geometry of the model was checked with PROCHECK (Laskowski et al., 1993), and all residues were found in allowed regions of the Ramachandran plot.

Circular Dichroism Spectroscopy

CD measurements were performed using an AVIV model 62DS spectropolarimeter, with a thermostated cuvette of 1 cm path length. All proteins were prepared in concentrations ranging from 1 μM to 2.5 μM in 10 mM NaPi (pH 8.0), 50 mM KCl, and 0.1 mM DTT. The average CD spectra were determined from five recorded wavelength scans (250–202 nm) at 4°C with a signal-averaging time of 3 s and then by subtraction of the background from a buffer blank. The CD spectra were decomposed with CDFit (http://www-structure.llnl.gov). Thermal unfolding curves were obtained by monitoring the ellipticity at 222 nm at temperatures ranging from 4°C–65°C in 1°C steps, with an equilibration time of 2 min at each step.

Protein Interaction Assays

GST fusions of various Sir4 protein fragments were expressed and purified from *E. coli* and used for pull-down assays to measure their interactions with Sir3 and Sir2. A minor species with a molecular weight of 70 KDa was copurified with GST-Sir4-C3. This was identified by mass spectrometry as the *E. coli* molecular chaperone DnaK, which we believe is bound to Sir4-C3 (Moazed et al., 1997). The fusion proteins were affinity purified on glutathione agarose beads and left coupled to the beads. Purified full-length Sir3 or truncated Sir3T, Sir2, or BSA was then added to the beads, and the mixtures were incubated at 4°C for 1 hr in 1 ml of binding buffer (20 mM NaPi [pH 8.0], 500 mM NaCl, 5 mM DTT, 0.1% Nonidet P-40, and 1 mM EDTA) with continuous mixing by inversion of the tubes. The beads were recovered by centrifugation at 2000 rpm for 2 min, washed five times with 1 ml of binding buffer, and then resuspended in 20 μl of SDS-PAGE sample buffer to elute the bound proteins. The samples were denatured by heating, and the proteins in the complexes were visualized by SDS-PAGE and staining with Coomassie brilliant blue.

Sedimentation Analysis

Sedimentation equilibrium centrifugation experiments were performed with an XL-A analytical ultracentrifuge (Beckman, Palo Alto). The protein samples were exhaustively dialyzed before use against 20 mM NaPi (pH 8.0), 500 mM NaCl, 1 mM DTT, and 1 mM EDTA.

The proteins were centrifuged at 4°C at speeds of 12,000 and 20,000 rpm while monitoring the protein concentration by radial scans of the sample cell at spacings of 0.001 cm. At each speed, the equilibration of the sample was confirmed by checking that protein concentration gradients measured after 24 hr and 40 hr were superimposable. Partial specific volumes of 0.725 mg ml^{-1} for Sir4-C1 and 0.740 mg ml^{-1} for Sir3T were estimated from their amino acid sequences, and the density of the solvent was calculated from the solvent composition.

Isothermal Titration Calorimetry

Isothermal calorimetric titrations were carried out with an MCS ITC instrument (MicroCal). All samples were prepared in a buffer composed of 20 mM NaPi (pH 8.0), 200 mM NaCl, 5 mM DTT, and 1 mM EDTA. Proteins were quantitated from their absorbance at 280 nm where an absorbance of 1 AU corresponds to a protein concentration of 6.8 mg ml^{-1} (0.373 mM) for Sir4-C1 and 1.54 mg ml^{-1} (0.026 mM) for Sir3T. Samples were dialyzed overnight against the same buffer in order to avoid any buffer mixing artifacts. Solutions were degassed before the experiments. A 200 μM stock solution of Sir4-C1 was titrated into the sample cell containing 25 μM Sir3T protein held at 10°C. Each titration consisted of an initial 4.0 μl injection and 18 subsequent 15 μl injections. Heats of dilution were measured by diluting Sir4-C1 into sample buffer, and they are consistent with those observed at the end of the experimental titrations when Sir4-C1 is in excess (Figure 6). The binding data were analyzed with the model for a single set of identical binding sites in the Origin software package (Microcal) to obtain the binding constant, molar stoichiometry, and binding enthalpy, along with their standard errors for the fit to the data.

Acknowledgments

We thank Stephen Blacklow, Peggy C. Stolt, and Patrick O'Brien for advice and assistance with circular dichroism measurements and Henry Ho for assistance with centrifugation studies. We also thank Eric Toth, Laura Silvian, Tom Hollis, Brandt Eichman, Masato Kato, and the staff of the macromolecular crystallography resource at the National Synchrotron Light Source (Upton, NY) for help with X-ray data collection and analysis. This work was supported by grants from the National Institutes of Health (R01 GM52506 to T.E. and R01 GM61641 to D.M.) and the resources of the Harvard-Armenise Structural Biology Center. T.E. is grateful for the support of the Hsien Wu and Daisy Yen Wu Professorship at Harvard Medical School.

Received: February 5, 2003
Revised: March 11, 2003
Accepted: March 19, 2003
Published: June 3, 2003

References

Akey, D.L., Malashkevich, V.N., and Kim, P.S. (2001). Buried polar residues in coiled-coil interfaces. Biochemistry *40*, 6352–6360.

Alber, T. (1992). Structure of the leucine zipper. Curr. Opin. Genet. Dev. *2*, 205–210.

Aparicio, O.M., Billington, B.L., and Gottschling, D.E. (1991). Modifiers of position effect are shared between telomeric and silent mating-type loci in S. cerevisiae. Cell *66*, 1279–1287.

Arndt, K., Pelletier, J., Muller, K., Pluckthun, A., and Alber, T. (2002). Comparison of in vivo selection and rational design of heterodimeric coiled coils. Structure *10*, 1235–1248.

Bailey, S. (1994). The CCP4 suite—programs for protein crystallography. Acta Crystallogr. D Biol. Crystallogr. *50*, 760–763.

Brünger, A.T., Adams, P.D., Clore, G.M., DeLano, W.L., Gros, P., Grosse-Kunstleve, R.W., Jiang, J.S., Kuszewski, J., Nilges, M., Pannu, N.S., et al. (1998). Crystallography and NMR system: a new software suite for macromolecular structure determination. Acta Crystallogr. D Biol. Crystallogr. *54*, 905–921.

Burkhard, P., Kammerer, R.A., Steinmetz, M.O., Bourenkov, G.P., and Aebi, U. (2000). The coiled-coil trigger site of the rod domain of cortexillin I unveils a distinct network of interhelical and intrahelical salt bridges. Structure *8*, 223–230.

Burkhard, P., Stetefeld, J., and Strelkov, S.V. (2001). Coiled coils: a highly versatile protein folding motif. Trends Cell Biol. *11*, 82–88.

Carmen, A.A., Milne, L., and Grunstein, M. (2002). Acetylation of the yeast histone H4 N terminus regulates its binding to heterochromatin protein SIR3. J. Biol. Chem. *277*, 4778–4781.

Carson, M. (1997). Ribbons. Methods Enzymol. *277*, 493–505.

Cockell, M., Palladino, F., Laroche, T., Kyrion, G., Liu, C., Lustig, A.J., and Gasser, S.M. (1995). The carboxy termini of Sir4 and Rap1 affect Sir3 localization: evidence for a multicomponent complex required for yeast telomeric silencing. J. Cell Biol. *129*, 909–924.

Cowtan, K., and Main, P. (1996). Phase combination and cross validation in iterated density-modification calculation. Acta Crystallogr. D Biol. Crystallogr. *52*, 43–48.

Crick, F.H.C. (1953). The packing of alpha-helices: simple coiled coils. Acta Crystallogr. *6*, 689–697.

Gartenberg, M.R. (2000). The Sir proteins of Saccharomyces cerevisiae: mediators of transcriptional silencing and much more. Curr. Opin. Microbiol. *3*, 132–137.

Gasser, S.M., and Cockell, M.M. (2001). The molecular biology of the SIR proteins. Gene *279*, 1–16.

Ghidelli, S., Donze, D., Dhillon, N., and Kamakaka, R.T. (2001). Sir2p exists in two nucleosome-binding complexes with distinct deacetylase activities. EMBO J. *20*, 4522–4535.

Harbury, P.B., Zhang, T., Kim, P.S., and Alber, T. (1993). A switch between two-, three-, and four-stranded coiled coils in GCN4 leucine zipper mutants. Science *262*, 1401–1407.

Harbury, P.B., Kim, P.S., and Alber, T. (1994). Crystal structure of an isoleucine-zipper trimer. Nature *371*, 80–83.

Hecht, A., Laroche, T., Strahl-Bolsinger, S., Gasser, S.M., and Grunstein, M. (1995). Histone H3 and H4 N-termini interact with SIR3 and SIR4 proteins: a molecular model for the formation of heterochromatin in yeast. Cell *80*, 583–592.

Hecht, A., Strahl-Bolsinger, S., and Grunstein, M. (1996). Spreading of transcriptional repressor SIR3 from telomeric heterochromatin. Nature *383*, 92–96.

Hoppe, G.J., Tanny, J.C., Rudner, A.D., Gerber, S.A., Danaie, S., Gygi, S.P., and Moazed, D. (2002). Steps in assembly of silent chromatin in yeast: Sir3-independent binding of a Sir2/Sir4 complex to silencers and role for Sir2-dependent deacetylation. Mol. Cell. Biol. *22*, 4167–4180.

Imai, S., Armstrong, C.M., Kaeberlein, M., and Guarente, L. (2000). Transcriptional silencing and longevity protein Sir2 is an NAD-dependent histone deacetylase. Nature *403*, 795–800.

Ivy, J.M., Klar, A.J., and Hicks, J.B. (1986). Cloning and characterization of four SIR genes of Saccharomyces cerevisiae. Mol. Cell. Biol. *6*, 688–702.

Jelesarov, I., and Bosshard, H.R. (1999). Isothermal titration calorimetry and differential scanning calorimetry as complementary tools to investigate the energetics of biomolecular recognition. J. Mol. Recognit. *12*, 3–18.

Jones, T.A., Zou, J.Y., Cowan, S.W., and Kjeldgaard, M. (1991). Improved methods for building protein models in electron density maps and the location of errors in these models. Acta Crystallogr. A *47*, 110–119.

Kennedy, B.K., Austriaco, N.R., Jr., Zhang, J., and Guarente, L. (1995). Mutation in the silencing gene SIR4 can delay aging in S. cerevisiae. Cell *80*, 485–496.

Kirchmaier, A.L., and Rine, J. (2001). DNA replication-independent silencing in S. cerevisiae. Science *291*, 646–650.

Kohn, W.D., Mant, C.T., and Hodges, R.S. (1997). Alpha-helical protein assembly motifs. J. Biol. Chem. *272*, 2583–2586.

Ladbury, J.E., and Chowdhry, B.Z. (1996). Sensing the heat: the application of isothermal titration calorimetry to thermodynamic studies of biomolecular interactions. Chem. Biol. *3*, 791–801.

Landry, J., Sutton, A., Tafrov, S.T., Heller, R.C., Stebbins, J., Pillus, L., and Sternglanz, R. (2000). The silencing protein SIR2 and its

homologs are NAD-dependent protein deacetylases. Proc. Natl. Acad. Sci. USA *97*, 5807–5811.

Laskowski, R.A., MacArthur, M.W., Moss, D.S., and Thornton, U.M. (1993). PROCHECK: a program to check the stereochemical quality of protein structures. J. Appl. Crystallogr. *26*, 283–291.

Leavitt, S., and Freire, E. (2001). Direct measurement of protein binding energetics by isothermal titration calorimetry. Curr. Opin. Struct. Biol. *11*, 560–566.

Li, Y.C., Cheng, T.H., and Gartenberg, M.R. (2001). Establishment of transcriptional silencing in the absence of DNA replication. Science *291*, 650–653.

Luo, K., Vega-Palas, M.A., and Grunstein, M. (2002). Rap1-Sir4 binding independent of other Sir, yKu, or histone interactions initiates the assembly of telomeric heterochromatin in yeast. Genes Dev. *16*, 1528–1539.

Marshall, M., Mahoney, D., Rose, A., Hicks, J.B., and Broach, J.R. (1987). Functional domains of SIR4, a gene required for position effect regulation in Saccharomyces cerevisiae. Mol. Cell. Biol. *7*, 4441–4452.

Marti, D.N., Jelesarov, I., and Bosshard, H.R. (2000). Interhelical ion pairing in coiled coils: solution structure of a heterodimeric leucine zipper and determination of pKa values of Glu side chains. Biochemistry *39*, 12804–12818.

Martin, S.G., Laroche, T., Suka, N., Grunstein, M., and Gasser, S.M. (1999). Relocalization of telomeric Ku and SIR proteins in response to DNA strand breaks in yeast. Cell *97*, 621–633.

McAinsh, A.D., Scott-Drew, S., Murray, J.A., and Jackson, S.P. (1999). DNA damage triggers disruption of telomeric silencing and Mec1p-dependent relocation of Sir3p. Curr. Biol. *9*, 963–966.

Miller, A.M., Sternglanz, R., and Nasmyth, K.A. (1984). The role of DNA replication in the repression of the yeast mating-type silent loci. Cold Spring Harb. Symp. Quant. Biol. *49*, 105–113.

Mills, K.D., Sinclair, D.A., and Guarente, L. (1999). MEC1-dependent redistribution of the Sir3 silencing protein from telomeres to DNA double-strand breaks. Cell *97*, 609–620.

Moazed, D. (2001). Common themes in mechanisms of gene silencing. Mol. Cell *8*, 489–498.

Moazed, D., and Johnson, D. (1996). A deubiquitinating enzyme interacts with SIR4 and regulates silencing in S. cerevisiae. Cell *86*, 667–677.

Moazed, D., Kistler, A., Axelrod, A., Rine, J., and Johnson, A.D. (1997). Silent information regulator protein complexes in Saccharomyces cerevisiae: a SIR2/SIR4 complex and evidence for a regulatory domain in SIR4 that inhibits its interaction with SIR3. Proc. Natl. Acad. Sci. USA *94*, 2186–2191.

Moretti, P., and Shore, D. (2001). Multiple interactions in Sir protein recruitment by Rap1p at silencers and telomeres in yeast. Mol. Cell. Biol. *21*, 8082–8094.

Moretti, P., Freeman, K., Coodly, L., and Shore, D. (1994). Evidence that a complex of SIR proteins interacts with the silencer and telomere-binding protein RAP1. Genes Dev. *8*, 2257–2269.

Murshudov, G.N., Vagin, A.A., and Dodson, E.J. (1997). Refinement of macromolecular structures by the maximum-likelihood method. Acta Crystallogr. D Biol. Crystallogr. *53*, 240–255.

O'Shea, E.K., Klemm, J.D., Kim, P.S., and Alber, T. (1991). X-ray structure of the GCN4 leucine zipper, a two-stranded, parallel coiled coil. Science *254*, 539–544.

Otwinowski, Z., and Minor, W. (1997). Processing of X-ray diffraction data collected in oscillation mode. Methods Enzymol. *276*, 307–326.

Palladino, F., Laroche, T., Gilson, E., Axelrod, A., Pillus, L., and Gasser, S.M. (1993). SIR3 and SIR4 proteins are required for the positioning and integrity of yeast telomeres. Cell *75*, 543–555.

Park, Y., Hanish, J., and Lustig, A.J. (1998). Sir3p domains involved in the initiation of telomeric silencing in Saccharomyces cerevisiae. Genetics *150*, 977–986.

Renauld, H., Aparicio, O.M., Zierath, P.D., Billington, B.L., Chhablani, S.K., and Gottschling, D.E. (1993). Silent domains are assembled continuously from the telomere and are defined by promoter distance and strength, and by SIR3 dosage. Genes Dev. *7*, 1133–1145.

Rine, J., and Herskowitz, I. (1987). Four genes responsible for a position effect on expression from HML and HMR in Saccharomyces cerevisiae. Genetics *116*, 9–22.

Rusche, L.N., Kirchmaier, A.L., and Rine, J. (2002). Ordered nucleation and spreading of silenced chromatin in Saccharomyces cerevisiae. Mol. Biol. Cell *13*, 2207–2222.

Smith, J.S., Brachmann, C.B., Celic, I., Kenna, M.A., Muhammad, S., Starai, V.J., Avalos, J.L., Escalante-Semerena, J.C., Grubmeyer, C., Wolberger, C., et al. (2000). A phylogenetically conserved NAD+-dependent protein deacetylase activity in the Sir2 protein family. Proc. Natl. Acad. Sci. USA *97*, 6658–6663.

Strahl-Bolsinger, S., Hecht, A., Luo, K., and Grunstein, M. (1997). SIR2 and SIR4 interactions differ in core and extended telomeric heterochromatin in yeast. Genes Dev. *11*, 83–93.

Tanner, K.G., Landry, J., Sternglanz, R., and Denu, J.M. (2000). Silent information regulator 2 family of NAD-dependent histone/protein deacetylases generates a unique product, 1-O-acetyl-ADP-ribose. Proc. Natl. Acad. Sci. USA *97*, 14178–14182.

Tanny, J.C., and Moazed, D. (2001). Coupling of histone deacetylation to NAD breakdown by the yeast silencing protein Sir2: evidence for acetyl transfer from substrate to an NAD breakdown product. Proc. Natl. Acad. Sci. USA *98*, 415–420.

Terwilliger, T.C., and Berendzen, J. (1999). Automated MAD and MIR structure solution. Acta Crystallogr. D Biol. Crystallogr. *55*, 849–861.

Tsukamoto, Y., Kato, J., and Ikeda, H. (1997). Silencing factors participate in DNA repair and recombination in Saccharomyces cerevisiae. Nature *388*, 900–903.

Van Duyne, G.D., Standaert, R.F., Karplus, P.A., Schreiber, S.L., and Clardy, J. (1993). Atomic structures of the human immunophilin FKBP-12 complexes with FK506 and rapamycin. J. Mol. Biol. *229*, 105–124.

Wyrick, J.J., Holstege, F.C., Jennings, E.G., Causton, H.C., Shore, D., Grunstein, M., Lander, E.S., and Young, R.A. (1999). Chromosomal landscape of nucleosome-dependent gene expression and silencing in yeast. Nature *402*, 418–421.

Accession Numbers

Coordinates have been deposited in the Protein Data Bank under accession code 1NYH.